Ionic-liquid lubrication of a nickel-based coating reinforced with tungsten carbide particles

N. Rivera[1], A. García[2,*], R. González[1,4], A. Fernández-González[3], A. Hernández Battez[2,4], M. Cadenas[2]

[1] Department of Marine Science and Technology, University of Oviedo, Asturias, Spain
[2] Department of Construction and Manufacturing Engineering, University of Oviedo, Gijón, Asturias, Spain
[3] Department of Physical and Analytical Chemistry, University of Oviedo, Asturias, Spain
[4] Department of Design and Engineering, Bournemouth University, Poole, BH12 5BB, UK

*Email: garciamaralberto@uniovi.es

Abstract

Trihexyltetradecylphosphonium bis(2-ethylhexyl)phosphate ([$P_{6,6,6,14}$][BEHP]) and trihexyltetradecylphosphonium bis(trifluoromethylsulfonyl)imide ([$P_{6,6,6,14}$][NTf_2]) ionic liquids were used as neat lubricants in nickel-based coatings reinforced with spherical WC particles (sizes: −106+45 μm). Three different coatings with 0, 3.3, and 12.4 wt% of WC on the surfaces were tested. Reciprocating tribological tests were performed (load: 100 N, frequency: 25 Hz, stroke length: 4 mm, for 60 min at room temperature). The wear was not related to the WC content for [$P_{6,6,6,14}$][BEHP]. However, the wear decreased with the increase in WC content when [$P_{6,6,6,14}$][NTf_2] was used. [$P_{6,6,6,14}$][BEHP] exhibited a better tribological behaviour than [$P_{6,6,6,14}$][NTf_2], particularly in the coating without WC, owing to the formation of a CrO_3 protective layer. Compared with [$P_{6,6,6,14}$][NTf_2], [$P_{6,6,6,14}$][BEHP] slightly worsened the antifriction and antiwear behaviour of the coatings with the decrease in WC content.

Keywords: ionic liquid; lubrication; NiCrBSi+WC coating; laser cladding

1. Introduction

Ni-based alloys are widely used in tribological pairs as hardfacing coatings owing to their antiwear and anticorrosion behaviour. The NiCrBSi alloys provide coatings with high tenacities, hardnesses, and protection against corrosion, depending on the Cr content [1]. The laser technology is one of the most recommended techniques for the fabrication of these coatings owing to the good control of the energy supplied during the manufacturing and relatively good industrial implementation of the process [2, 3], making the laser cladding one of the most advantageous techniques. The laser cladding is an industrial process in which the powder material of the coating and thin surface layer of the substrate are initially simultaneously melted under laser irradiation and then

rapidly solidified to form a coating with a metallurgical bond to the substrate material with a minimum dilution of the clad layer. The wear resistance of the NiCrBSi alloy coating can be increased by the addition of hard particles such as hard nonfused carbides. Tungsten carbide is one of the most used materials in the reinforcement of NiCrBSi coatings [4]. The higher hardness of the WC particles and their thermal stability provide good tribological behaviours under different dry conditions: abrasive wear [5], sliding, abrasive and erosive wear [6], and high-temperature wear [7].

On the other hand, few studies have been carried out on the improvement in antiwear behaviours of coatings using liquid lubrication. Stewart et al. [8] studied the rolling contact fatigue of a post-treated WC-NiCrBSi functionally graded thermal spray coating under full and mixed lubrication conditions using two commercial high-viscosity hydrocarbon lubricants. The improvement in the tribological behaviour of a NiCrBSi laser cladding coating was also studied under mixed lubrication conditions using a nanofluid as the lubricant [9] and under the combination of laser texturing and liquid lubrication [10].

The use of ionic liquids (ILs) as lubricants has been generally studied in steel–steel contacts, and less studied using other materials. Aluminium–steel [11] and Ni-alloy–steel [12] tribopairs were studied using different ILs as neat lubricants. CrN, TiN, and diamond-like carbon coatings obtained by physical vapour deposition were tested under liquid lubrication using different ILs [13–17], while the combination of Ni-based+WC laser cladding coatings and ILs has not been studied.

The number of studies on the use of the ILs in lubrication has increased since 2001 owing to their excellent lubrication properties [18–21]. However, they lead to solubility problems in nonpolar oils, which has been overcome with the use of phosphonium-cation-based ILs with long alkyl chains [22, 23]. However, all phosphonium-cation-

based ILs are not fully miscible in nonpolar oils, and thus the tribological behaviours of some of them have been tested as neat lubricants in steel–steel pairs [24]. In addition, the use of coatings in mechanical systems to reduce friction and wear can be improved using a liquid lubricant as a complementary lubrication system.

The aim of this study was to analyse the tribological performances of two phosphonium-cation-based ILs: trihexyltetradecylphosphonium bis(2-ethylhexyl)phosphate ($[P_{6,6,6,14}][BEHP]$) and trihexyltetradecylphosphonium bis(trifluoromethylsulfonyl)imide ($[P_{6,6,6,14}][NTf_2]$), as neat lubricants for WC-NiCrBSi coatings with different WC contents (0, 3.3, and 12.4 wt% of WC). Dry sliding tribological behavior of these coatings has been studied by authors in a previous research work [25]. The novelty of the present study is the combined use of ILs and anti-wear hard coatings in order to improve the tribological behavior of the latter.

2. Experimental methods

2.1. Materials

Commercially available NiCrBSi powder (Metco 12C) and spherical tungsten carbide powder (Woka 50054) were used for the manufacturing of the coatings over an AISI 1045 carbon steel substrate. Three different WC contents were studied, 0, 3.3, and 12.4 wt% of WC, measured on the test surface of the coating. The WC percentages were determined by analysing optical microscopy images of the surfaces. Three areas of each coating were etched with Nital + Murakami, and then the volume fraction of carbides was measured using an image processing software identifying the regions of carbides by means of the colour tone and counting the total number of pixels for these regions. Finally, the weight percentage was calculated using the measured volume fraction and densities of both matrix phase and WC particles [25]. A Rofin Sinar CO_2 laser with a

Precitec YC-50M coaxial cladding head was used. The laser cladding parameters and detailed study on the microstructures of these coatings are reported in Refs. [25–27]. The addition of WC particles generates an increase in hardness of the matrix phase of the coating owing to the diffusion of tungsten towards the matrix phase [27]. Table 1 shows the microhardness of the matrix phase.

Table 1. Microhardness of the matrix phase and roughnesses of the coatings.

Coating	**Hardness**	**Roughness (*Ra*)**
NiCrBSi	500 HV_1	0.8 µm
NiCrBSi + 3.3% WC	515 $HV_{0.1}$	0.8 µm
NiCrBSi + 12.4% WC	526 $HV_{0.1}$	0.8 µm

The physicochemical properties of the ILs used as neat lubricants in this study are summarized in Table 2. Both ILs have purities of 98%. The CAS number of $[P_{6,6,6,14}][BEHP]$ is 1092655-30-5, while its empirical formula is $C_{48}H_{102}O_4P_2$. The CAS number of $[P_{6,6,6,14}][NTf_2]$ is 460092-03-9, while its empirical formula is $C_{34}H_{68}F_6NO_4PS_2$. We previously analysed the thermal stabilities of the ILs [24].

Table 2. Physicochemical properties of the ILs.

IUPAC* name	**Acronym**	**Water content, KF** (%)**	**Density at 20 °C ($g \cdot cm^{-3}$)**	**Viscosity (mPa·s)**		**Viscosity index**
				40 °C	**100 °C**	
Trihexyltetradecylphosphonium bis(2-ethylhexyl)phosphate	$[P_{6,6,6,14}][BEHP]$	≤ 0.5	0.9116	474.3	50.8	181
Trihexyltetradecylphosphonium bis(trifluoromethylsulfonyl) imide	$[P_{6,6,6,14}][NTf_2]$	≤ 0.05	1.0711	130.4	16.4	140

* International Union of Pure and Applied Chemistry ** Karl Fischer

2.2. Tribological tests

Reciprocating friction and wear tests were carried out using a Bruker UMT-3 microtribometer in a ball-on-flat configuration. A normal load of 100 N was applied using a closed-loop servomechanism, recording the normal and tangential forces (normal and friction forces). Room-temperature tests were performed for 60 min using a stroke length of 4 mm and frequency of 25 Hz. The IL (25 μL) was introduced on the coated surface before the tribological tests. The coated surface (flat) and ball (composed of WC, diameter: 9.5 mm, hardness: 90.5 HRA) were cleaned with heptane for 5 min in an ultrasonic bath and then hot-air-dried. Three replicates of tests were carried out for each coating–IL combination.

2.3. Surface characterisation

To measure the wear volume after the tribological test and study the chemical interactions between the ILs and coatings, several techniques such as confocal microscopy, scanning electron microscopy (SEM), energy-dispersive spectroscopy (EDS), and X-ray photoelectron spectroscopy (XPS) were used. Confocal microscopy (Leica DCM 3d) was used to scan the topography of the wear scar. A JEOL- 6610LV SE microscope with an integrated INCA Energy 350 - Xmax 50 ED spectrometer was used for the surface analysis. The XPS experiments were carried out with a SPECS spectrometer using a monochromatic Al K_α X-ray source (1486.74 eV) in the focus mode at 125 W. The dimensions of the spot were 3.5×0.2 mm^2, focused on the wear scar. A pass energy of 30 eV was selected for high-resolution spectra, whereas a pass energy of 90 eV was used for survey spectra. The analyser electromagnetic lens mode was “small area”, while the scan mode was “fixed analyser transmission”.

3. Results and discussion

3.1. Friction and wear results

The evolution of the coefficient of friction (COF) during the most representative tribological test for each coating–IL combination is shown in Fig. 1. The COFs remained stable after the test time of 300 s.

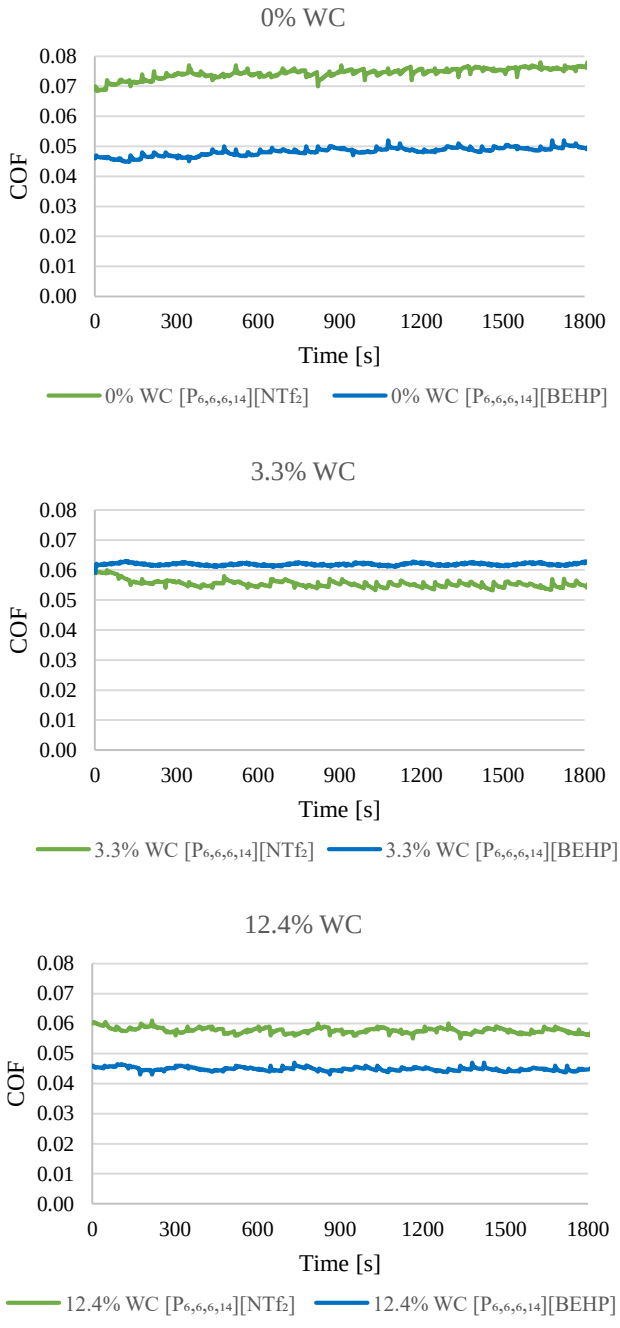

Fig. 1. Evolutions of the COFs during the tribological tests.

Fig. 2 shows the mean friction behaviour of each combination of coating–IL. The use of the $[P_{6,6,6,14}][BEHP]$ IL reduced the friction, compared to the case with $[P_{6,6,6,14}][NTf_2]$, when the coating without WC reinforcement particles was used. This result is different from that obtained for the steel–steel pair under very similar test conditions, where the friction behaviours obtained using the two ILs were similar [24]. The inclusion of WC particles in the NiCrBSi coating reduced the friction only when $[P_{6,6,6,14}][NTf_2]$ was used as the lubricant. On the contrary, the use of $[P_{6,6,6,14}][BEHP]$ combined with WC reinforcement particles in the coating did not change the friction behaviour, with respect to the nonreinforced coating. The variability of COF measurements when $[P_{6,6,6,14}][BEHP]$ was used combined to 3.3% of WC is greater than the differences between COF values using the same IL and different WC contents and as a result, these differences in COF are not significant. In general, no considerable difference in friction was observed between the reinforced coatings with the same WC concentration. In general, the coatings with 12.4% of WC exhibited lower friction mean values and deviations than those of the other coatings.

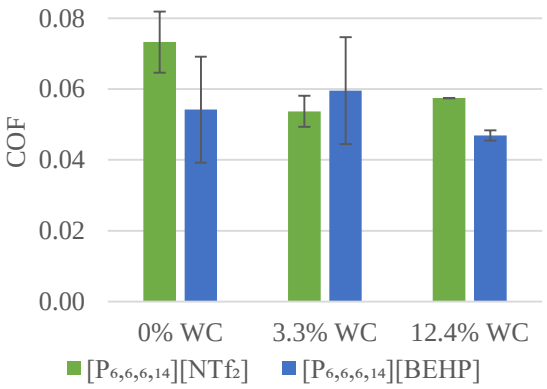

Fig. 2. Friction behaviour of each coating–IL combination.

The wear behaviour of each coating–IL combination is shown in Fig. 3. The wear volume was measured by scanning the wear scar using the confocal microscope. Similar to the friction results, the coating without WC lubricated with the $[P_{6,6,6,14}][BEHP]$ IL exhibited a lower wear than that obtained with the $[P_{6,6,6,14}][NTf_2]$ lubricant. The lubrication with $[P_{6,6,6,14}][NTf_2]$ did not change the linear decrease in wear with the increase in WC content. On the contrary, the coating lubricated with the $[P_{6,6,6,14}][BEHP]$ IL exhibited a considerable wear reduction only when the WC content was 12.4%.

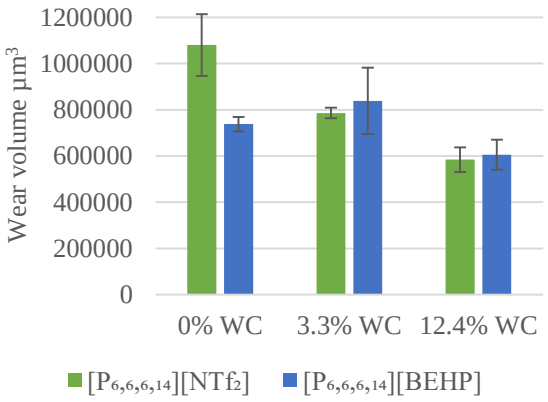

Fig. 3. Wear volumes measured on the coated surfaces.

The samples without WC reinforcement exhibited a large difference in wear volume; even a similar value to that for the coating with 3.3% of WC was observed when $[P_{6,6,6,14}][BEHP]$ was used as the lubricant. This could be related to the formation of a CrO_3 protective layer [28], Table 3, which could not be detected in the samples lubricated with $[P_{6,6,6,14}][NTf_2]$. On the other hand, the presence of WC particles in the coating increased its hardness and reduced wear, as it was found under dry sliding conditions [25, 27]. This hardness increase seems to be more important than the formation of CrO_3 found in the WC-containing coatings (Table 3), where their

corresponding wear values are similar at equal WC content (Fig. 3).

3.2. Analysis of the worn surfaces

Figs. 4 and 5 show images of the wear scars on the coated specimens. The unmelted spherical WC particles of the coating can be observed. According to a previous study [27], the microstructures of these coatings are composed of γ-Ni dendrites (240 $HV_{0.005}$) and eutectic structure (940 $HV_{0.025}$), which becomes finer with the increase in percentage of WC particles. A slight dilution of WC particles at the edges and refinement of the eutectic structure of the matrix phase near the WC particles were detected. Consequently, complex carbides, mainly W_2C and chromium carbides, precipitate in the matrix phase and thus the average hardness of the matrix increases with the content of WC particles. The increase in average hardness of the coating matrix explains the main observed wear behaviour, i.e., with the increase in percentage of WC particles, the wears generally decrease for both ILs used as lubricants.

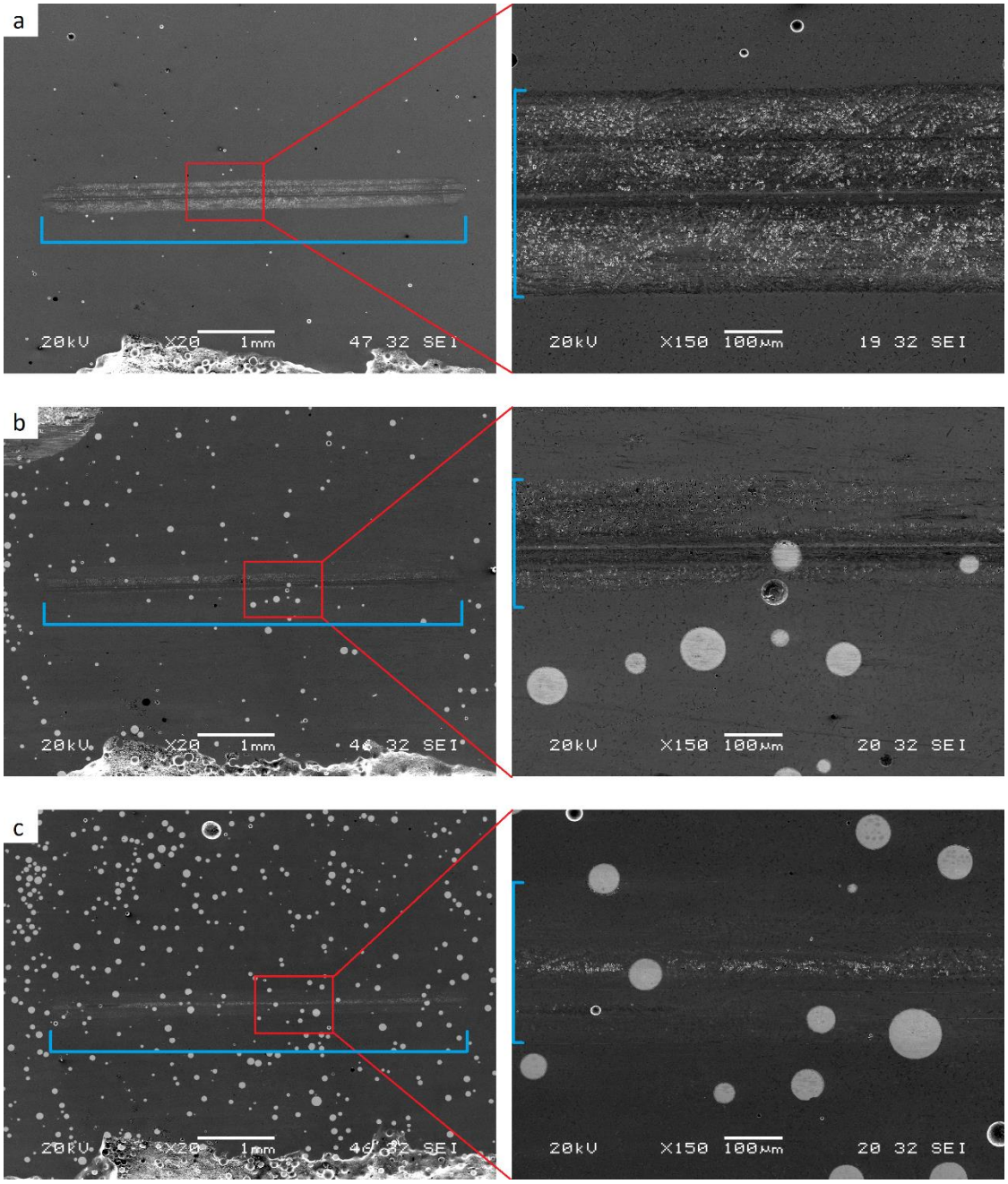

Fig. 4. SEM images of the wear scars for the structures with $[P_{6,6,6,14}][BEHP]$:

a) 0, b) 3.3, and c) 12.4 wt% of WC.

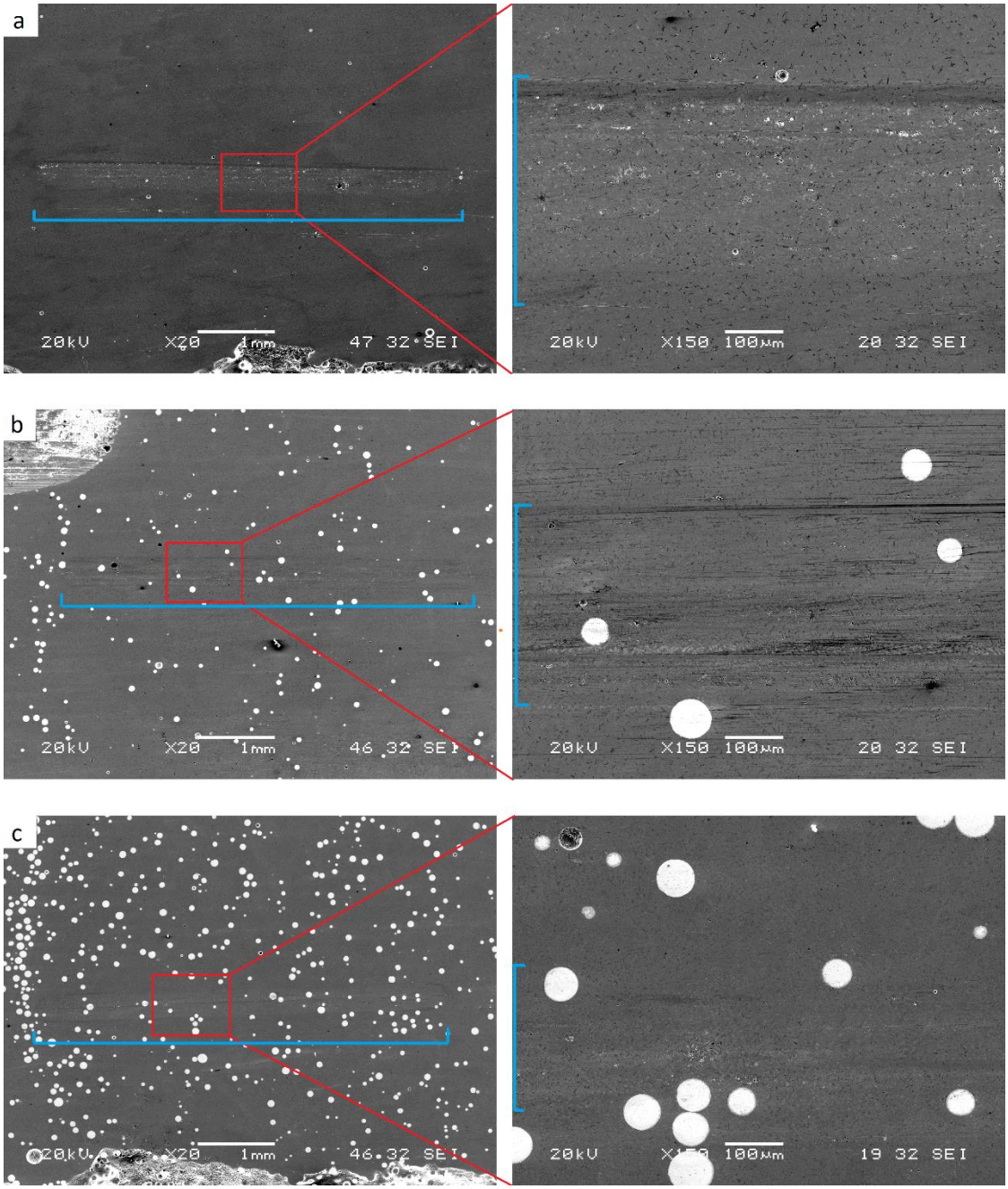

Fig. 5. SEM images of the wear scars for the structures with $[P_{6,6,6,14}][NTf_2]$: a) 0, b) 3.3, and c) 12.4 wt% of WC.

Figs. 4 and 5 also show that the WC particles are not damaged (fractured carbides are not observed), indicating the absence of the three-body abrasive wear mechanism, which was observed when these coatings were tested under dry sliding conditions [25].

The wear track widths are larger in the coatings without WC because of their lower hardnesses, and thus their larger contact area under a similar normal load. Figs. 4a and 5a show a larger wear scar on the coating lubricated with $[P_{6,6,6,14}][NTf_2]$, consistent with the wear volume measured using the confocal microscope.

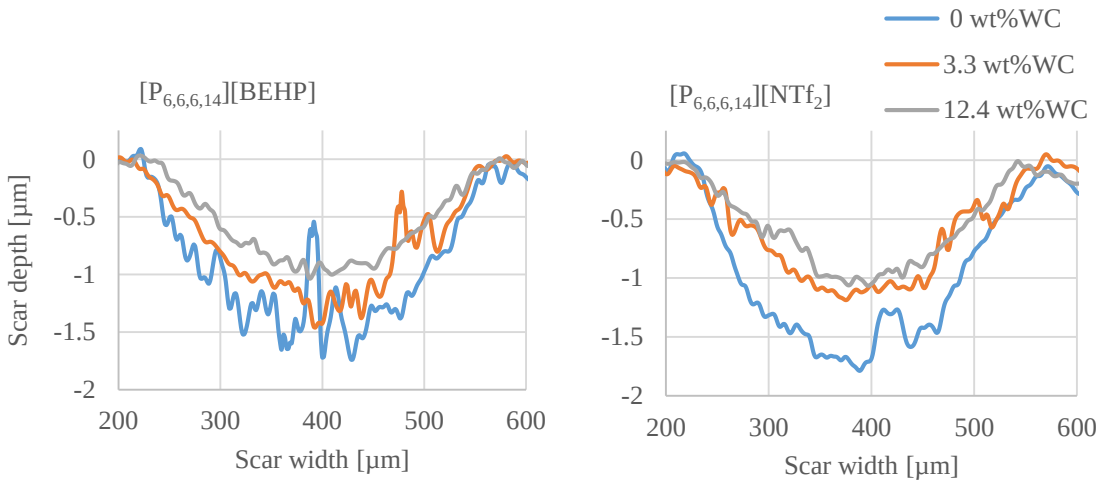

Fig. 6. Profiles of the wear scars of the samples shown in Figs. 4 and 5.

Fig. 6 shows the profiles of the wear scars in Figs. 4 and 5. Each profile was measured at the middle of the corresponding wear track. The scar depth of the sample without WC particles lubricated with $[P_{6,6,6,14}][NTf_2]$ is considerably larger than those of the samples with 3.3% and 12.4% of WC and those of all samples lubricated with $[P_{6,6,6,14}][BEHP]$, as expected according to the measured wear volumes. In addition, higher roughness was observed inside the wear scars of the samples without WC particles, particularly in the sample lubricated with $[P_{6,6,6,14}][BEHP]$.

Fig. 7 shows the EDS results for two areas of the coating, inside and outside the wear track. The analysis shows no considerable changes in the composition of the coating after the tribological test; the spectra are similar. The main elements in the coating correspond to its composition: Ni, Cr, B, Si, and Fe of the matrix and W and C of the

WC particles. In Fig. 7, W and C are not observed as the wear scar is on the sample without WC particles. Boron is not detected owing to its low atomic number. The EDS technique has a depth of surface analysis in the order of microns, and consequently does not allow to adequately evaluate the tribofilms, which are in the order of nanometres. The emissions of the elements in the tribolayer having a low thickness are masked by the emissions of the elements under the tribolayer.

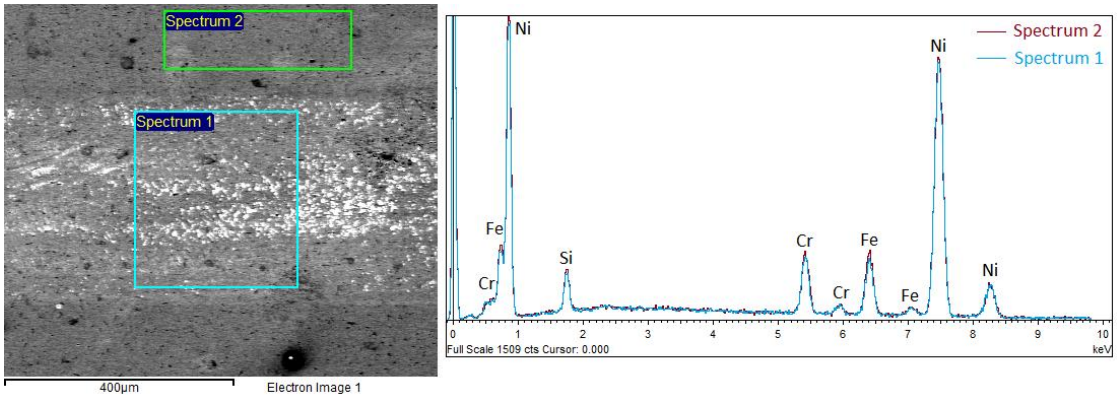

Fig. 7. EDS analysis of the sample without WC lubricated with $[P_{6,6,6,14}][BEHP]$ inside (Spectrum 1) and outside (Spectrum 2) the wear scar.

The XPS technique could be used for the detection of compounds with a smaller depth of penetration in the surface, and thus enables a more detailed analysis of the formed tribofilms. An XPS analysis of the wear scar was carried out, recording the spectra of Ni, C, and O. W could not be easily detected in the samples as its amount was below the limit of detection. Likewise, fluorine and phosphorus could not be detected. Therefore, the detected carbon should not be related to the WC but to other sources of carbon, mostly the IL. For the surfaces lubricated with $[P_{6,6,6,14}][NTf_2]$ (Fig. 8), the O/Ni ratios are equal for all coatings, while the C/Ni ratios are slightly higher at the surfaces with 3.3% and 12.4% of WC. This indicates a higher content of carbon from the IL in the wear scar, which seems to be consistent with the lower measured COF.

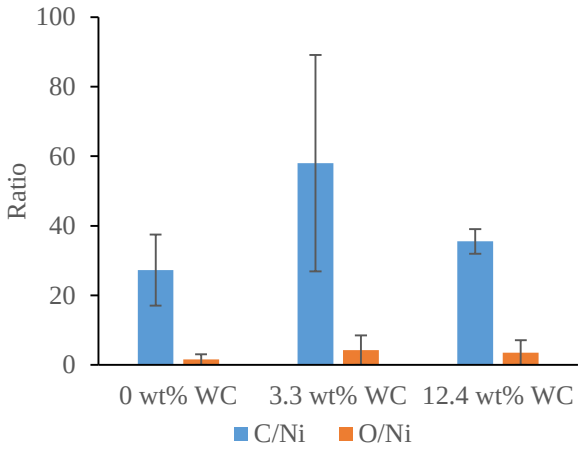

Fig. 8. C/Ni and O/Ni ratios on the wear scars for the samples lubricated with $[P_{6,6,6,14}][NTf_2]$.

The high-resolution spectrum of the Ni $2p_{3/2}$ band shows three peaks for each sample (Fig. 9), at 852.1 ± 0.5, 854.6 ± 0.4, and 855.9 ± 0.5 eV assigned to metallic Ni, NiO, and Ni_2O_3, respectively [29]. Most of the nickel is unoxidised (70 ± 2%); similar nickel contents are observed in both nickel oxides (14 ± 3% for Ni_2O_3 and 17 ± 3% for NiO). In addition, no significant differences in the percentages are observed between the samples. On the other hand, the high-resolution spectra of chromium revealed differences between the surfaces (Fig. 10). Table 3 shows that the sample without WC exhibits two Cr $2p_{3/2}$ peaks at 574.1 (~34%) and 576.8 (~66%) eV, assigned to metallic chromium and Cr_2O_3, respectively [30, 31]. For the sample with 3.3 wt% of WC, an additional peak at 575.3 eV is observed, which agrees with that corresponding to chromium carbide [32] (ratios: 40% (carbide), 35% (Cr), and 25% (oxide)).

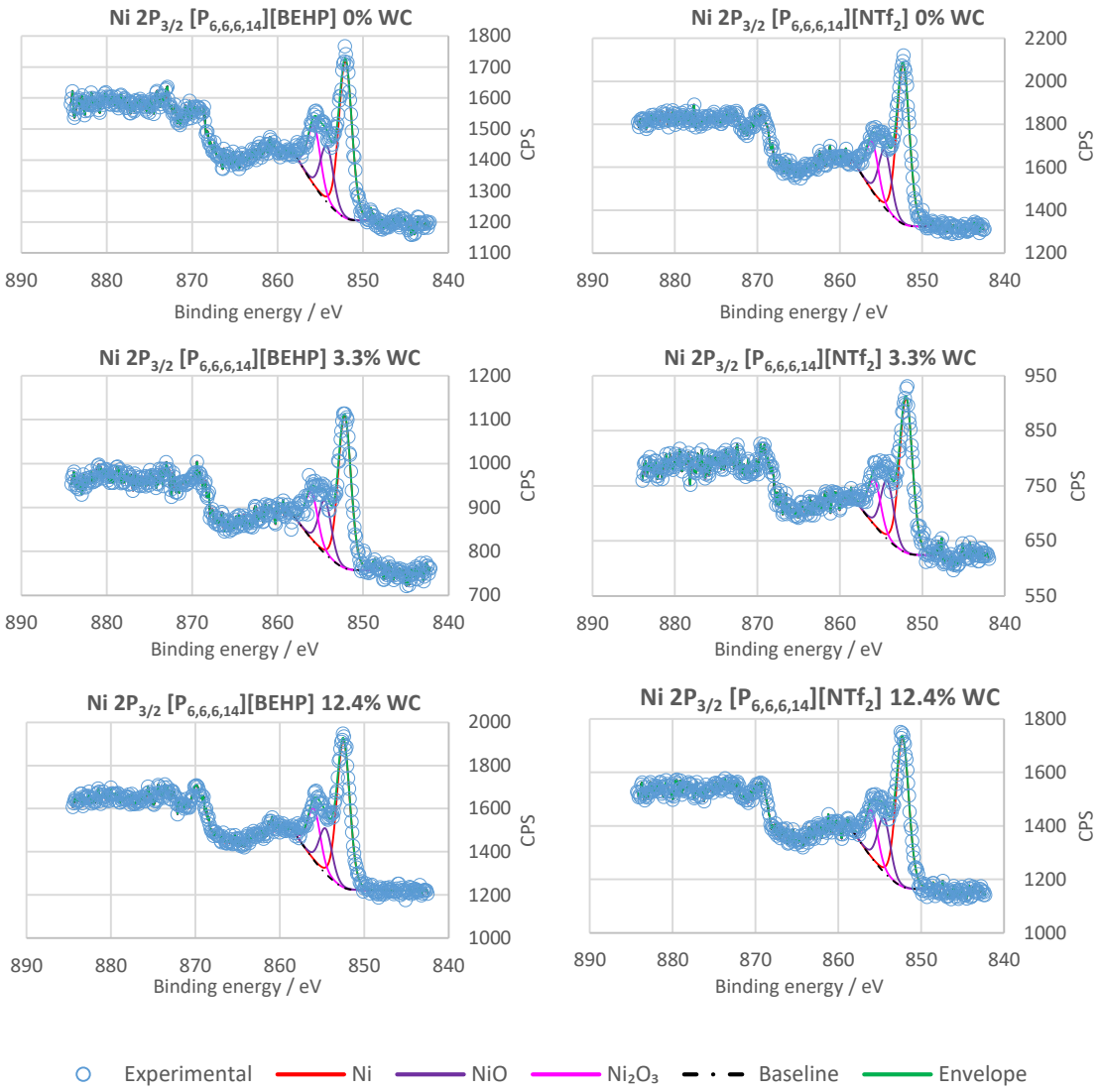

Fig. 9. Ni 2$p_{3/2}$ spectra.

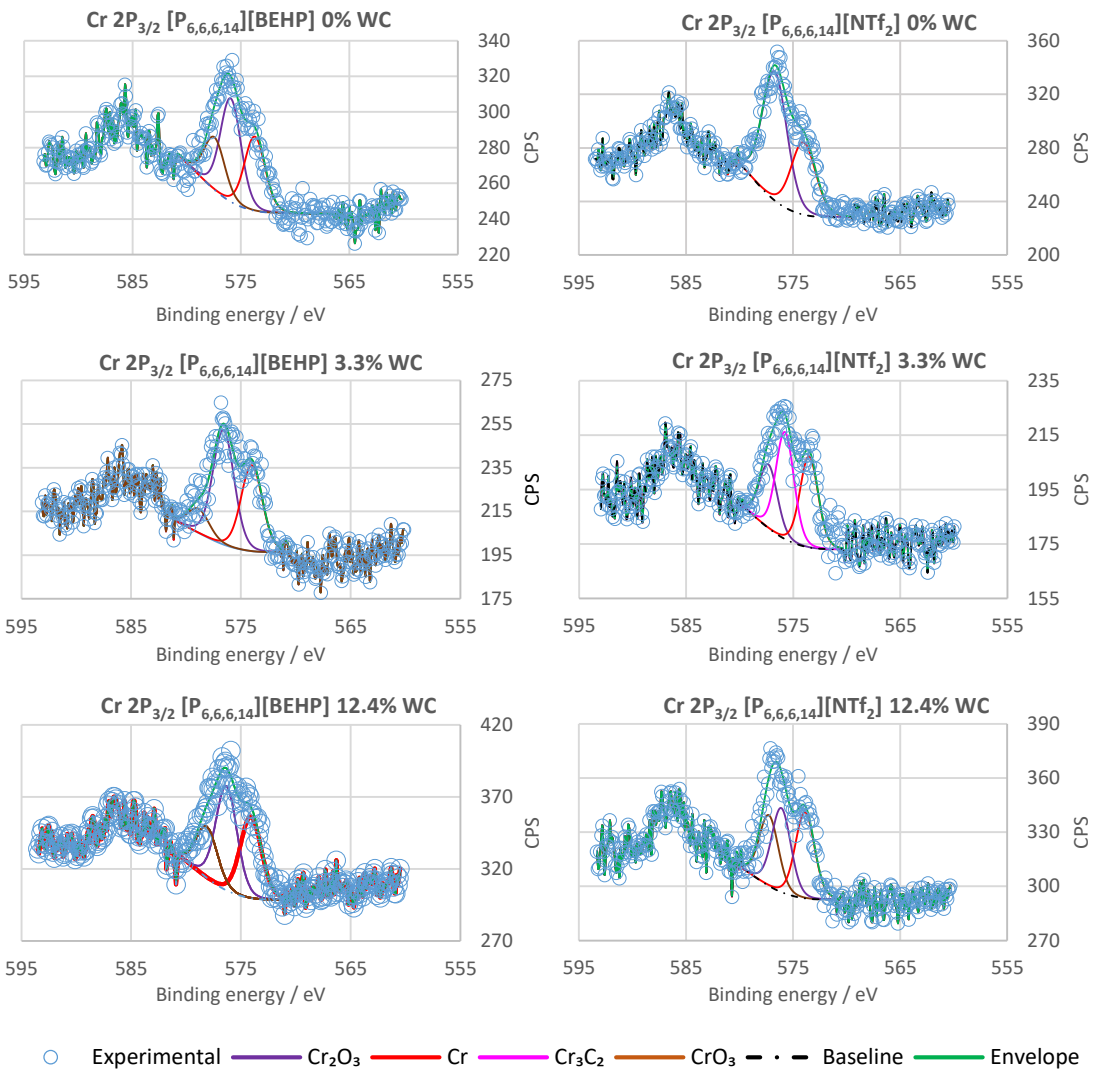

Fig. 10. Cr $2p_{3/2}$ spectra.

It is worth noting that the analysis depth in XPS is a few nanometres, whereas that in SEM is a few micrometres. Therefore, the apparent discrepancy in the content of oxygen between the two techniques can be explained considering the very thin layer (few nanometres), which can be detected by XPS, but is masked by the raw material during the EDS analysis.

In the case with the $[P_{6,6,6,14}][BEHP]$ IL, no significant variation in the C/Ni ratio is observed, as in the case with $[P_{6,6,6,14}][NTf_2]$, which could explain the very similar

tribological behaviours of the three different coatings (Figs. 2 and 3). Likewise, the high-resolution analysis of the Cr $2p_{3/2}$ peak did not reveal significant differences. Three peaks were observed in each case, at 573.9, 576.4, and 578.5 eV, assigned to metallic chromium, Cr_2O_3, and probably to highly oxidised forms of chromium such as CrO_3, respectively [33].

CrO_3 is not detected in the samples without WC and 3.3 wt% WC lubricated with $[P_{6,6,6,14}][NTf_2]$. The CrO_3 observed when $[P_{6,6,6,14}]$[BEHP] was used could explain the better friction and wear behaviours of the coating without WC. When the WC-reinforced coatings are used, the tribological behaviours are attributed to the combination of the CrO_3 protective layer [28] and proper WC content. A careful analysis should be carried out as Cr (VI) is a toxic and potentially carcinogenic compound [34].

Regarding the absence of CrO_3 in the samples lubricated with $[P_{6,6,6,14}][NTf_2]$ and 0 wt% and 3.3 wt% WC coatings, these results suggest that the higher oxidation states of chromium are achieved only in the samples with the highest wt% of WC. Thus, 0 wt% and 3.3 wt% WC coatings show chromium in oxidation states (OS) 0, II and III, whereas the OS VI appears only in the 12.4 wt% WC coating.

Table 3. Peak positions (eV) in the high-resolution spectra of Cr $2p_{3/2}$.

	0 wt% of WC	**3.3 wt% of WC**	**12.4 wt% of WC**
$[P_{6,6,6,14}][NTf_2]$	574.1 (Cr) 576.8 (Cr_2O_3)	573.1 (Cr) 575.3 (Cr_3C_2) 577.3 (Cr_2O_3)	574.1 (Cr) 576.7 (Cr_2O_3) 578.6 (CrO_3)
$[P_{6,6,6,14}]$[BEHP]	573.7 (Cr) 576.2 (Cr_2O_3) 578.3 (CrO_3)	573.9 (Cr) 576.6 (Cr_2O_3) 578.9 (CrO_3)	574.1 (Cr) 576.5 (Cr_2O_3) 578.3 (CrO_3)

4. Conclusions

The conclusions of this study can be summarised as follows:

- When the $[P_{6,6,6,14}][BEHP]$ IL was used as the neat lubricant, the wears of the coatings were similar irrespective of the WC content. When the $[P_{6,6,6,14}][NTf_2]$ IL was used, the tribological behaviour of the coating was improved with the increase in WC content. This could be related to the higher viscosity of $[P_{6,6,6,14}][BEHP]$.
- The combination of the 12.4%-WC-containing coating and $[P_{6,6,6,14}][BEHP]$ IL exhibited the best tribological behaviour (lowest friction and wear).
- The $[P_{6,6,6,14}][BEHP]$ IL provided better friction and wear reduction behaviours than those of $[P_{6,6,6,14}][NTf_2]$, particularly in the coating without WC, owing to the formation of the CrO_3 tribofilm.
- Compared with $[P_{6,6,6,14}][NTf_2]$, the $[P_{6,6,6,14}][BEHP]$ IL slightly worsened the antifriction and antiwear behaviours of the NiCrBSi + WC coating with the decrease in WC content.

Acknowledgements

The authors thank the Ministry of Economy and Competitiveness (Spain) and Foundation for the Promotion of Applied Scientific Research and Technology in Asturias (FICYT) for the support for this study within the framework of the research projects DESCARTA (DPI2010-15285), STARLUBE (DPI2013-48348-C2-1-R), and LUSUTEC (FC-GRUPIN-IDI/2018/000131).

References

[1] I. Hemmati, V. Ocelík, J. Th. M. De Hosson, Effects of the alloy composition on phase constitution and properties of laser deposited Ni-Cr-B-Si coatings, Physics Procedia 41 (2013) 302-311. https://doi.org/10.1016/j.phpro.2013.03.082

[2] R. Gonzalez, M.A. Garcia, I. Peñuelas, M. Cadenas, M. del Rocio Fernandez, A. Hernández, D. Felgueroso, Microstructural study of NiCrBSi coatings obtained by different processes, Wear 263 (2007) 619-624. https://doi.org/10.1016/j.wear.2007.01.094

[3] A. García, M. Cadenas, M.R. Fernández, A. Noriega, Tribological effects of the geometrical properties of plasma spray coatings partially melted by laser, Wear 305 (2013) 1-7. https://doi.org/10.1016/j.wear.2013.05.004

[4] M.J. Tobar, C. Alvarez, J.M. Amado, G. Rodríguez, A. Yañez, Morphology and characterization of laser clad composite NiCrBSi–WC coatings on stainless steel, Surf. Coat. Technol. 200 (2006) 6313-6317. https://doi.org/10.1016/j.surfcoat.2005.11.093

[5] Z. Kamdi, P.H. Shipway, K.T. Voisey, A.J. Sturgeon, Abrasive wear behaviour of conventional and large-particle tungsten carbide-based cermet coatings as a function of abrasive size and type, Wear 271 (2011) 1264–1272. https://doi.org/10.1016/j.wear.2010.12.060

[6] M. Antonov, I. Hussainova, Cermets surface transformation under erosive and abrasive wear, Tribol. Int. 43 (2010) 1566–1575. https://doi.org/10.1016/j.triboint.2009.12.005

[7] C. Guo, J. Zhou, J. Chen, J. Zhao, Y. Yu, H. Zhou, High temperature wear resistance of laser cladding NiCrBSi and NiCrBSi/WC–Ni composite coatings, Wear 270 (2011) 492–498. https://doi.org/10.1016/j.wear.2011.01.003

[8] S. Stewart, R. Ahmed, T. Itsukaichi, Contact fatigue failure evaluation of post-treated WC–NiCrBSi functionally graded thermal spray coatings, Wear 257 (2004) 962-983. https://doi.org/10.1016/j.wear.2004.05.008

[9] A. Hernández Battez, J.L. Viesca, R. González, D. Blanco, E. Asedegbega, A. Osorio, Friction reduction properties of a CuO nanolubricant used as lubricant for a NiCrBSi coating, Wear 268 (2010) 325–328. https://doi.org/10.1016/j.wear.2009.08.018

[10] A. Higuera Garrido, R. González, M. Cadenas, A. Hernández Battez, Tribological behavior of laser-textured NiCrBSi coatings, Wear 271 (2011) 925–933. https://doi.org/10.1016/j.wear.2011.03.027

[11] J. Qu, J. J. Truhan, S. Dai, H. LuoP., J. Blau, Ionic liquids with ammonium cations as lubricants or additives, Tribol. Lett. 22 (2006) 207-214. https://doi.org/10.1007/s11249-006-9081-0

[12] A.E.Jiménez, M.D.Bermúdez, P.Iglesias, Lubrication of Inconel 600 with ionic liquids at high temperature, Tribol. Int.42 (2009) 1744-1751. https://doi.org/10.1016/j.triboint.2008.11.004

[13] A. Hernández Battez, R. González, J.L. Viesca, A. Fernández-González, M. Hadfield, Lubrication of PVD coatings with ethyl-dimethyl-2-methoxyethylammonium tris(pentafluoroethyl)trifluorophosphate, Tribol. Int. 58 (2013) 71-78. https://doi.org/10.1016/j.triboint.2012.10.001

[14] R. González, A. Hernández Battez, J.L. Viesca, A. H. Garrido, A. Fernández-González, Lubrication of DLC coatings with two tris(pentafluoroethyl)trifluorophosphate anion-based ionic liquids, Tribol. Trans.56 (2013) 887-895. https://doi.org/10.1080/10402004.2013.810319

[15] D. Blanco, R. González, A. Hernández Battez, J.L. Viesca, A. Fernández-González, Use of ethyl-dimethyl-2-methoxyethylammonium tris(pentafluoroethyl)trifluorophosphate as base oil additive in the lubrication of TiN PVD coating, Tribol. Int. 44 (2011) 645-650. https://doi.org/10.1016/j.triboint.2011.01.004

[16] D. Blanco, A. Hernández Battez, J. L. Viesca, R. González and A. Fernández-González, Lubrication of CrN Coating With Ethyl-Dimethyl-2-Methoxyethylammonium Tris(pentafluoroethyl)Trifluorophosphate Ionic Liquid as Additive to PAO 6, Tribol. Letters 41 (2011) 295-302. https://doi.org/10.1007/s11249-010-9714-1

[17] R. González, A. Hernández Battez, D. Blanco, J. L. Viesca, A. Fernández-González, Lubrication of TiN, CrN and DLC PVD Coatings with 1-Butyl-1-Methylpyrrolidinium tris(pentafluoroethyl)trifluorophosphate, Tribology Lett. 40 (2010) 269-277. https://doi.org/10.1007/s11249-010-9674-5

[18] C. Ye, W. Liu, Y. Chen, L. Yu, Room-temperature ionic liquids: a novel versatile lubricant, Chem Commun (Camb) (2001) 2244–2245. https://doi.org/10.1039/B106935G

[19] M.D. Bermúdez, AE. Jiménez, J. Sanes, F.J. Carrión, Ionic liquids as advanced lubricant fluids, Molecules 14 (2009) 2888–2908. https://doi.org/10.3390/molecules14082888

[20] I. Minami, Ionic liquids in tribology, Molecules 14 (2009) 2286–2305. https://doi.org/10.3390/molecules14062286

[21] A. Somers, P. Howlett, D. MacFarlane, M. Forsyth, A review of ionic liquid lubricants, Lubricants 1 (2013) 3–21. https://doi.org/10.3390/lubricants1010003

[22] Y. Zhou, J. Qu, Ionic Liquids as Lubricant Additives: A Review, ACS Appl. Mater. Interfaces, 9, 4 (2017) 3209–3222. https://doi.org/10.1021/acsami.6b12489

[23] R. González, M. Bartolomé, D. Blanco, J.L. Viesca, A. Fernández-González, A. Hernández Battez, Effectiveness of phosphonium cation-based ionic liquids as lubricant additive, Tribol. Int. 98 (2016) 82-93. https://doi.org/10.1016/j.triboint.2016.02.016

[24] A. Hernández Battez, M. Bartolomé, D. Blanco, J.L. Viesca, A. Fernández-González, R. González, Phosphonium cation-based ionic liquids as neat lubricants: Physicochemical and tribological performance, Tribol. Int. 95 (2016) 118–131. https://doi.org/10.1016/j.triboint.2015.11.015

[25] M.R. Fernández, A. García, J.M. Cuetos, R. González, A. Noriega, M. Cadenas, Effect of actual WC content on the reciprocating of a laser cladding NiCrBSi alloy reinforced with WC, Wear 324-325 (2015) 80–89. https://doi.org/10.1016/j.wear.2014.12.021

[26] A. García, M.R. Fernández, J.M. Cuetos, R. González, A. Ortiz, M. Cadenas, Study of the sliding wear and friction behavior of WC+NiCrBSi laser cladding coatings as a function of actual concentration of WC reinforcement particles in ball on disk test, Tribol. Lett. 63 (2016) 41. https://doi.org/10.1007/s11249-016-0734-3

[27] A. Ortiz, A. García, M. Cadenas, M.R. Fernández, J.M. Cuetos, WC particles distribution model in the cross-section of laser cladded NiCrBSi + WC coatings, for different wt% WC, Surf. Coat. Technol. 324 (2017) 298-306. https://doi.org/10.1016/j.surfcoat.2017.05.086

[28] H. C. Barshilia, B. Deepthi, K.S. Rajam, Transition Metal Nitride–Based nanolayered Multilayer Coatings and Nanocomposite Coatings as Novel Superhard, in: S. Zhang (Eds.), Nanostructured Thin Films and Coatings: Mechanical Properties, Volume 1, CRC Taylor & Francis, Boca Raton FL, 2010, 446-446. https://doi.org/10.1201/b11764

[29] H.S. Maharana, A. Basu, K. Mondal, Structural and tribological correlation of electrodeposited solid lubricating Ni-WSe_2 composite coating, Surf. Coat. Technol. 349 (2018) 328–339. https://doi.org/10.1016/j.surfcoat.2018.06.005

[30] T.P. Moffat, R.M. Latanision, R.R. Ruf, An X-ray photoelectron spectroscopy study of chromium-metalloid alloys—III, Electrochim. Acta 40-11 (1995) 1723-1734. https://doi.org/10.1016/0013-4686(95)00015-7

[31] Z. Luan, M. Zhang, K. Chen, The investigation for the deactivation mechanism of Cu-Cr impregnated carbon by XPS, Carbon 31-7 (1993) 1179-1784. https://doi.org/10.1016/0008-6223(93)90070-Q

[32] X. Liu, S. Zhang, Y. Li, Green preparation of in situ Cr_3C_2 nano-coatings on graphite surface and their water-wettability and rheological properties, Ceram. Int. 44-8 (2018) 9526-9533. https://doi.org/10.1016/j.ceramint.2018.02.172

[33] G.P. Halada, C.R. Clayton, Photoreduction of Hexavalent Chromium during X-Ray Photoelectron Spectroscopy Analysis of Electrochemical and Thermal Films, J. Electrochem. Soc. 138-10 (1991) 2921-2927. https://doi.org/10.1149/1.2085340

[34] WHO Regional Office for Europe, Chapter 6.4 *Chromium* in: Air Quality Guidelines, 2nd edition, Coppenhagen, Denmark, 2000. http://www.euro.who.int/__data/assets/pdf_file/0017/123074/AQG2ndEd_6_4Chromium.PDF